Segmental Strain for Scar Detection in Acute Myocardial Infarcts and in Follow-up Exams using Non-Contrast CMR Cine Sequences

Malgorzata Polacin (Malgorzata.Polacin@usz.ch)
University of Zurich
Mihaly Karolyi
University of Zurich
Matthias Eberhard
University of Zurich
Ioannis Matziris
University of Zurich
Hatem Alkadhi
University of Zurich
Sebastian Kozerke
University and ETH Zurich
Robert Manka
University of Zurich

Research Article

Keywords: cardiac magnetic resonance, acute myocardial infarction, ischemic heart disease, feature tracking

Posted Date: August 20th, 2021

DOI: https://doi.org/10.21203/rs.3.rs-685378/v1

Abstract

Background

The purpose of the study was to investigate feasibility of infarct detection in segmental strain derived from non-contrast cardiac magnetic resonance (CMR) cine sequences in patients with acute myocardial infarction (AMI) and in follow-up (FU) exams.

Methods

57 patients with AMI (mean age 61 ± 12 years, CMR 2.8 ± 2 days after infarction) were retrospectively included, FU exams were available in 32 patients (35 ± 14 days after first CMR). 28 patients with normal CMR (47 ± 8 years) served as controls. Dedicated software (Segment CMR, Medviso) was used to calculate global and segmental strain derived from cine sequences. Cine short axis stacks and segmental circumferential strain calculations of every patient and control were presented to two blinded readers in random order, who were advised to identify potentially infarcted segments, blinded to LGE and clinical information.

Results

Impaired global strain was measured in AMI patients compared to controls (global peak circumferential strain [GPCS] p= 0.01; global peak longitudinal strain [GPLS] p= 0.04; global peak radial strain [GPRS] p= 0.01). In both imaging time points, mean segmental peak circumferential strain [SPCS] was impaired in infarcted tissue compared to remote segments (AMI: p=0.03, FU: p=0.02). SPCS values in infarcted segments were similar between AMI and FU (p=0.8), remote segments were marginally more impaired in AMI than in FU (p= 0.07). In SPCS calculations, 141 from 189 acutely infarcted segments were accurately detected (74.6%), visual evaluation of correlating cine images detected 44.4% infarcts. In FU, 81.5 % infarcted segments (93/114 segments) were detected in SPCS and 51.8% by visual evaluation of correlating short axis cine images (p=0.01).

Conclusion

Segmental circumferential strain derived from routinely acquired native cine sequences detects nearly 75 % of acute infarcts and about 80% of infarcts in subacute follow-up CMR, significantly more than visual evaluation of correlating cine images alone. Acute infarcts may display only subtle impairment of wall motion and no obvious wall thinning, thus SPCS calculation might be helpful for scar detection in patients with acute infarcts, when only cine images are available.

Background

Upon myocardial infarction, scar tissue is best visualized by cardiac magnetic resonance imaging (CMR) with late gadolinium enhancement (LGE) [1]. Intravenous application of gadolinium-based contrast agents is mandatory before acquiring LGE sequences. However, gadolinium should be used carefully in

some patient groups, such as patients with severely reduced kidney function. Gadolinium-free options for the detection of ischemic myocardial scars are limited. One promising alternative is scar detection using regional myocardial deformation parameters [2, 3]. Myocardial deformation during cardiac contraction can be quantified by myocardial feature tracking (FT) based on routinely acquired, non-contrast cine sequences [4, 5]. Necrosis of myocytes after myocardial infarction with subsequent scar replacement disturbs mechanical properties of the myocardium with consecutively altered global and segmental strain [6]. Especially chronic myocardial scars with wall thinning and noticeable wall motion abnormality result in significant segmental strain impairment, which can be used to distinguish scar tissue from remote myocardium [2, 3, 7]. In contrast, acute infarcts might lack significant myocardial wall thinning and display less wall motion abnormalities in cine images. Therefore, the impact of acute and subacute infarcts on segmental strain needs to be further analyzed. In this study, global and segmental strain derived from non-contrast cine images was analyzed in patients with acute myocardial infarction (AMI) and in subacute follow-up (FU) exams and the practicability of using segmental strain for scar detection in both exams was investigated.

Methods

Study population

From July 2019 until December 2020 57 patients (15 female, mean age 61 ± 12 years) with AMI in CMR (imaging 2.8 ± 2 days [range 0–6 days] after reperfusion therapy) were retrospectively assessed. Thirty-two out of 57 patients had a FU exam (35 ± 14 days, [range 20–86 days]).

Patients with concomitant primary cardiomyopathies (n = 2) or non-diagnostic LGE images (n = 3) were not enrolled. Twenty-eight individuals (2 female, mean age 48 ± 10 years) with normal CMR examinations during the same time period were also retrospectively included. CMR referrals in the control group were exclusion of structural heart disease (n = 4) or exclusion of coronary artery disease (n = 24). Demographic characteristics of patients and controls are shown in Table 1.

CMR data acquisition

CMR exams were acquired on a 1.5T MR (Achieva, Philips Healthcare). Cine balanced steady-state free precession (SSFP) images in long-axis geometries (2-, 3- and 4-chamber view) and in short axis orientation covering the entire left ventricle (LV) (field of view: 350 × 350 mm^2; matrix: 300 × 300; repetition time/echo time: 3.0/1.5 ms; in-plane resolution 1.2 × 1.2 mm^2; number of cardiac phases: 50; section thickness: 8 mm) were acquired for functional assessment of the LV. Edema-sensitive black-blood T2-weighted images with fat saturation in five short axis slices were acquired for visualization of myocardial edema [8]. Fifteen minutes after administration of gadolinium (0.2 mmol gadobutrol

[Gadovist; Bayer Schering Pharma, Zurich, Switzerland] per kilogram body weight), LGE (inversion recovery gradient-echo sequence; field of view: 350 × 350 mm^2; matrix: 234 × 234; repetition time/echo time: 7.4/4.4 ms; inversion time: 205–255 ms; flip angle: 20°; in-plane resolution: 1.5 × 1.5 mm^2; section thickness: 8 mm) was performed in short axis and in 2-,3- and 4 chamber view.

CMR Data analysis

Strain analysis – Dedicated software (Segment v3.0 R7946, Medviso, Lund, Sweden) was used to calculate global and segmental strain derived from native cine sequences as previously described [3]. Duration of data loading, image registration, contouring of myocardial borders and strain calculation was 10 min 17 s ± 43 s (range 9 min 15 s – 11 min 31 s) per patient or control, respectively. Blinded to patient information (patient or control) and to LGE images, all strain analyses were performed be one reader (reader A: five years of experience in cardiac imaging). Interobserver agreement was performed on 28 random cases by a second reader due to the semi-automatic nature of strain analyses (reader B: two years of experience in cardiac imaging, blinded to the results of reader A).

Infarct detection in circumferential strain calculations and in cine images – Reader A and B were advised to identify possibly infarcted segments in segmental circumferential strain calculations (right column of Fig. 1a und 1b) as well as in the corresponding short axis cine images, visually recognizing wall motion abnormalities (VWMA) as previously described [3]. Datasets of all patients (AMI and FU exams) and controls were mixed and presented in random order to both readers. Both readers were blinded to each other, to LGE/edema images (Fig. 1a and 1b, left column) and to clinical information.

Assessment of infarcted segments in LGE images – In a separate session, both readers had to select affected segments (short axis stack LGE, black-blood T2-weighted images with fat saturation) blinded to clinical information. Reference standard was the existing corresponding report (revised by a cardiologist with over 15 years of experience in CMR). Ventricular volumes and function were calculated using IntelliSpace Portal, performed by reader A (Philips, Version 8.0.3) (Table 1).

Statistical analyses

Statistics were performed using commercially available software (IBM SPSS Statistics, release 25.0; SPSS, Armonk, NY). Categoric data are expressed as numbers or percentages and quantitative data are expressed as means ± standard deviations. Normal distribution was tested by the Kolmogorov–Smirnov test. Two-tailed paired *t*-tests or Wilcoxon signed rank were used to compare global and segmental strain values as well as to compare infarcted segments found in LGE, circumferential strain calculations and by visual wall motion assessment. Interobserver agreement was investigated using the intraclass correlation coefficient (ICC). ICC = 0.50–0.75 was considered moderate, ICC = 0.75–0.9 was considered good and ICC > 0.9 was considered excellent agreement [9]. Receiver operating characteristics (ROC) were calculated to determine the cut-offs of segmental strain values and area under the curve (AUC) for segmental circumferential strain in order to differentiate infarcted from remote myocardium. ROC curve analysis was not performed for segmental longitudinal or radial strain due to lacking significance

between strain values in infarcted and remote myocardium. Statistical significance was supposed at a p-value below 0.05.

Results

LGE and edema

In patients with acute infarction, 189 out of 896 segments showed LGE (21.1%) and myocardial edema. Myocardial edema was also detected in 27 segments without LGE. Mean scar burden per patient was 23.4% ± 6 (range 8–59%) and the average amount of infarcted segments per patient was 3.7 (range: 2–9).

In the subgroup of patients with follow-up exams 118 out of 512 segments showed LGE (23 %). Scar burden at acute imaging timepoint was 25.1% ± 5 per patient (range 12–56%) along with myocardial edema, further 10 segments had myocardial edema without concomitant LGE. Scar burden decreased in follow-up exams (20.7 ± 4, range 5–48%) (Table 1). No LGE was found in the control group.

Global strain

In patients, mean global strain was impaired compared to controls (global peak circumferential strain [GPCS]: -10.3% ± 3 vs. 20.1% ± 2, p = 0.01; global peak longitudinal strain [GPLS]: -10.7 % ± 5 vs. 18.6 % ± 2 p = 0.04; global peak radial strain strain [GPRS]: 27.9% ± 5 vs. 39.2% ± 5; p = 0.01, Fig. 2). In the subgroup with follow-up CMR, similar mean global strain values were measured between both time points (GPCS: -10.6% ± 2 vs. -9.5 % ± 3, p = 0.7; GPLS − 10.2 % ± 5 vs. 10.9 % ± 5 p = 0.8; GPRS 26.8% ± 6 vs. 29.8% ± 4; p = 0.2; Fig. 2).

Segmental strain

Segmental strain in patients with AMI

In patients with AMI, impaired mean segmental peak circumferential strain (SPCS) was measured in infarcted segments compared to mean SPCS of healthy myocardium (-10.5% ± 1, p = 0.03) (Fig. 3), interobserver agreement was excellent (Table 2*).* Mean segmental peak longitudinal strain (SPLS) and mean segmental peak radial strain (SPRS) in infarcted segments were mildly impaired (SPLS − 6.5 % ± 8 and SPRS 15.9% ± 7) compared to SPLS and SPRS of remote myocardium (SPLS − 11.8% ± 5 and SPRS 23.4% ± 7, p = 0.7 and 0.5) (Fig. 3). From 189 segments with LGE, 141 could be identified in cine based segmental circumferential strain calculations (ICC 0.869, 95%CI: 0.811–0.908). Moreover, both readers detected all patients with scars in strain calculations, the “missed” 48 segments belonged to patients, that were already diagnosed with at least one infarcted segment. 15 segments were assumed “infarcted” in circumferential strain calculations without displaying LGE, all those segments had myocardial oedema. Visual assessment of wall motion abnormalities (VWMA) in cine images revealed 84 infarcted segments out of 189 (44,4%; ICC 0.783, 95%CI: 0.727–0.819) (Fig. 4). No normal segments (without oedema and

LGE) in patients nor segments in controls were assumed infarcted by VWMA or circumferential strain calculations.

Segmental strain in follow-up MRI

In FU exams, mean SPCS and SPRS were also significantly impaired in infarcted segments compared to SPCS and SPRS of remote myocardium (SPCS − 2.4% ± 2 vs.-13.4% ± 2, p = 0.02; SPRS 16.7% ± 4 vs. 32.4% ± 3, p = 0.02; Fig. 3) with excellent interobserver agreement (Table 2*)*. Direct comparison between imaging in the acute setting and in follow-up CMR revealed no significant differences in segmental strain values between infarcted segments and remote myocardium, however, a tendency towards lower segmental circumferential strain of remote myocardium in the acute subgroup was noticeable (AMI − 10.6% ± 1 vs. FU exam − 12.9% ± 2, p = 0.07; Fig. 3). Since segmental circumferential strain appeared to be suitable for identifying segments with ischemic scars, we performed ROC analysis to detect the optimal cut-off values for SPCS for discrimination of infarcted segments and remote myocardium. For our patient group, segments with SPCS below 5,9 % (sensitivity of 86,2 %, specificity of 83,5%, AUC 0,89 [0,878–0,923]; Fig. 5*)* is considered infarcted. Evaluation of segmental circumferential strain calculations detected 93 out of 114 infarcted segments (81,6%; ICC 0.871, 95%CI: 0.811–0.915), detection of VWMA in cine sequences revealed 59 segments (51,8%; ICC 0.802, 95%CI: 0.759–0.831) (Fig. 4). Both readers missed one patient with subtle subendocardial scar (one infarcted segment) in segmental circumferential strain calculation.

Discussion

This study analyzed the feasibility of using segmental strain for scar detection in patients with acute myocardial infarcts and in subacute follow-up exams.

Intravenous application of gadolinium-based contrast agents is necessary to perform LGE sequences, the gold standard for scar imaging after myocardial infarction. However, patients with recent myocardial infarction may suffer from acute renal failure and application of gadolinium should be used restrictively in those cases. In the clinical setting, established alternatives for scar detection in native CMR sequences are limited. With native T1 mapping, scar and remote myocardium can be differentiated due to different tissue relaxation times [10, 11]. However, additional mapping sequences need to be acquired and in order to achieve accurate measurements and standardized parameters for healthy myocardium need to be defined separately for every scanner. Moreover, while acute infarcts can be reliably detected in native T1 maps, T1 values of infarcted areas normalize after acute infarction with resulting lower specificity for chronic infarcts [12]. Some artificial intelligence-based techniques successfully detected scar tissue in non-contrast cine CMR sequences [13, 14], but these methods are mostly still in a proof-of-concept stage and are not yet practicable in clinical use.

Myocardial feature tracking (FT) was introduced as a novel technique for myocardial strain quantification based on routinely acquired cine sequences. Infarcted tissue leads to altered global and segmental myocardial strain due to reduced contractility of fibroblasts, that gradually replace necrotic myocardium

after myocardial infarction [6]. Impairment of global strain in patients with acute and chronic infarcts have been reported by various studies [15, 16]. Accordingly, GPLS, GPRS and especially GPCS was impeded in our patient cohort compared to healthy controls. Studies analyzing segmental strain in patients with infarcts in the last decade revealed heterogenous results, in particular problems with accuracy and reproducibility of segmental strain values have been reported [17]. Newer algorithms for strain quantification based on non-rigid algorithm for image registration and segmentation with tracking of the whole image content - instead of tracking myocardial borders only- seem to accurately identify scarred myocardium in segmental circumferential strain [18, 19].

Chronic scars with wall motion abnormalities and myocardial wall thinning lead to severe impairment of segmental strain in contrast to healthy tissue, allowing distinction of remote and infarcted segments in strain measurements [2, 7]. However, the impact of acute infarcts - with more subtle wall motion abnormalities and without wall thinning - on segmental strain has not yet been sufficiently investigated.

In our patient cohort, mean SPCS in infarcted tissue was impaired compared to SPCS of remote myocardium and this was observed in both acute imaging as well as in follow-up CMRs; in ROC analyses cut-off value was – 5.9%, below which segments were considered infarcted.

Also direct comparison of wall motion and segmental circumferential strain calculations of every patient in a blinded dataset revealed markedly more infarcted segments in segmental circumferential strain calculations than by analyzing cine images only and this was true for the acute timepoint (74.6% vs. 44.4%) as well as in follow-up exams (81.5% vs. 52 %). Imaging in the early phase after myocardial infarction is challenging due to complex pathophysiologic processes of the acutely infarcted myocardium and compensatory mechanisms of adjacent remote tissue [20], nevertheless segmental circumferential strain was able to detect nearly 75% of acutely infarcted segments. Although some infarcted segments were not found by segmental circumferential strain calculations, not even one patient with acute infarction was missed and only one patient with small subendocardial scar was missed in the follow-up exam. Reduced scar burden was noticed in follow-up exams, most probably due to subsided edema [21]. More evident wall motion abnormality and incremental myocardial thinning weeks after infarction might be responsible for more infarcted segments detected by VWMA in the follow-up exam than in first CMR [22]. Interestingly, absolute global strain values were similar in both exams as well as segmental circumferential strain values in infarcted segments. Segmental circumferential strain in remote myocardium was slightly more impaired in the acute imaging timepoint and further analyses revealed, that edematous segments were mainly responsible for strain impairment, suggesting influence of myocardial edema on segmental circumferential strain.

In summary, segmental circumferential strain based on non-contrast cine images detects most ischemic scars in the acute timepoint and in subacute follow-up exams in contrast to visual evaluation of cine images and can potentially be used for scar identification. Since CMR based strain is increasingly established in clinical use, this method might be a promising problem solver in patients with ischemic heart disease who cannot receive or reject gadolinium or when LGE images are non-diagnostic.

Limitations

Some limitations must be mentioned. In this retrospective study of 57 patients, follow-up exams were available only in 32 individuals. The mean interval of 5 weeks between initial imaging and follow-up CMR is presumably not long enough to measure remodelling, because of still ongoing pathophysiologic processes and distant time points should be investigated for that matter in further studies. Since segmental circumferential strain calculations use the 16-segment model, apical infarction (segment 17) will not be detected in SPCS.

Although definition of scar transmurality is important in clinical setting, transmurality assessment in acutely infarcted myocardium might be challenging and was not performed in our study. Ultimately, strain measurements were performed with only one software. Recent studies show, that strain values are not interchangeable between different vendors, thus vendor-specific threshold values need to be defined for infarcted and remote myocardium [19].

Conclusion

Segmental circumferential strain derived from routinely acquired non-contrast cine sequences detects nearly 75 % of acute infarcts and about 80% of infarcts in subacute follow-up CMR, significantly more than visual evaluation of cine images alone. Especially in acute infarcts, where wall motion abnormalities may be subtle and wall thinning is not yet present, this technique may aid infarct detection in patients with ischemic heart disease, who cannot receive or reject gadolinium application or when LGE images are non-diagnostic.

Abbreviations

AMI: acute myocardial infarction; AUC: area under the curve; CMR: cardiac magnetic resonance; FT: feature tracking; FU: follow-up (exam)*;* GPCS: global peak circumferential strain; GPLS: global peak longitudinal strain; GPRS: global peak radial strain; ICC: intraclass correlation coefficient; i.v.: intravenous; *LGE: late gadolinium enhancement; LV: left ventricle/left-ventricular:* LVEDV: left ventricular end-diastolic volume; LVEF: left ventricular ejection fraction; LVESV: left ventricular end-systolic volume; LVSV: left ventricular stroke volume; ms: milliseconds; min: minute(s); ROC: receiver operating characteristics; s: seconds; SPCS: segmental peak circumferential strain; SPLS: segmental peak longitudinal strain; SPRS: segmental peak radial strain; SSFP: steady- state free precession; T: Tesla; VWMA : Visual wall motion abnormality

Declarations

Authors' Contributions:

M.P. and R.M. designed the study. M.P., M.K., M.E. and I.M. provided patient data and images. M.P. and M.K. performed data analysis. M.P. wrote the manuscript. M.E., H.A., S.K. and R.M. proofread the manuscript.

Funding

We received no funding for the study.

Availability of data and materials

The datasets generated and analysed during this study are not publicly available due to their patient referable character, thereby compromising individual privacy, but are available from the corresponding author on reasonable request.

Ethics approval and consent to participate

This retrospective study was conducted in accordance to the Declaration of Helsinki and its later amendments and the institutional review board approved this retrospective study (Cantonal ethics commission, Canton Zurich, BASEC-Nr. 2019-00808; commitee`s reference numer: not applicable). All participants gave written informed consent.

Consent for publication

Not applicable.

Acknowledgements

Not applicable.

Competing interests

The authors declare they have no competing interests.

References

1. Treibel TA, White SK, Moon JC. Myocardial Tissue Characterization: Histological and Pathophysiological Correlation. Curr Cardiovasc Imaging Rep 2014;7:1–9. https://doi.org/10.1007/s12410-013-9254-9.
2. Tantawy SW, Mohammad SA, Osman AM, El Mozy W, Ibrahim AS. Strain analysis using feature tracking cardiac magnetic resonance (FT-CMR) in the assessment of myocardial viability in chronic ischemic patients. Int J Cardiovasc Imaging 2020. https://doi.org/10.1007/s10554-020-02018-w.
3. Polacin M, Karolyi M, Eberhard M, Gotschy A, Baessler B, Alkadhi H, et al. Segmental strain analysis for the detection of chronic ischemic scars in non-contrast cardiac MRI cine images. Sci Rep 2021;11:1–11. https://doi.org/10.1038/s41598-021-90283-7.

4. Claus P, Omar AMS, Pedrizzetti G, Sengupta PP, Nagel E. Tissue Tracking Technology for Assessing Cardiac Mechanics: Principles, Normal Values, and Clinical Applications. JACC Cardiovasc Imaging 2015. https://doi.org/10.1016/j.jcmg.2015.11.001.
5. Pedrizzetti G, Claus P, Kilner PJ, Nagel E. Principles of cardiovascular magnetic resonance feature tracking and echocardiographic speckle tracking for informed clinical use. J Cardiovasc Magn Reson 2016. https://doi.org/10.1186/s12968-016-0269-7.
6. Richardson WJ, Clarke SA, Alexander Quinn T, Holmes JW. Physiological implications of myocardial scar structure. Compr Physiol 2015. https://doi.org/10.1002/cphy.c140067.
7. Zou Q, Zheng T, Zhou SL, Tang XP, Li SH, Zhou W, et al. Quantitative evaluation of myocardial strain after myocardial infarction with cardiovascular magnetic resonance tissue-tracking imaging. Int Heart J 2020;61:429–36. https://doi.org/10.1536/ihj.19-384.
8. Simonetti OP, Finn JP, White RD, Laub G, Henry DA. "Black blood" T2-weighted inversion-recovery MR imaging of the heart. Radiology 1996. https://doi.org/10.1148/radiology.199.1.8633172.
9. Koo TK, Li MY. A Guideline of Selecting and Reporting Intraclass Correlation Coefficients for Reliability Research. J Chiropr Med 2016. https://doi.org/10.1016/j.jcm.2016.02.012.
10. Taylor AJ, Salerno M, Dharmakumar R, Jerosch-Herold M. T1 Mapping Basic Techniques and Clinical Applications. JACC Cardiovasc Imaging 2016. https://doi.org/10.1016/j.jcmg.2015.11.005.
11. Thongsongsang R, Songsangjinda T, Tanapibunpon P, Krittayaphong R. Native T1 mapping and extracellular volume fraction for differentiation of myocardial diseases from normal CMR controls in routine clinical practice. BMC Cardiovasc Disord 2021;21:1–17. https://doi.org/10.1186/s12872-021-02086-3.
12. O H-Ici D, Jeuthe S, Al-Wakeel N, Berger F, Kuehne T, Kozerke S, et al. T1 mapping in ischaemic heart disease. Eur Heart J Cardiovasc Imaging 2014. https://doi.org/10.1093/ehjci/jeu024.
13. Zhang N, Yang G, Gao Z, Xu C, Zhang Y, Shi R, et al. Deep learning for diagnosis of chronic myocardial infarction on nonenhanced cardiac cine MRI. Radiology 2019. https://doi.org/10.1148/radiol.2019182304.
14. Baessler B, Mannil M, Oebel S, Maintz D, Alkadhi H, Manka R. Subacute and chronic left ventricular myocardial scar: Accuracy of texture analysis on nonenhanced cine MR images. Radiology 2018. https://doi.org/10.1148/radiol.2017170213.
15. Reindl M, Tiller C, Holzknecht M, Lechner I, Beck A, Plappert D, et al. Prognostic Implications of Global Longitudinal Strain by Feature-Tracking Cardiac Magnetic Resonance in ST-Elevation Myocardial Infarction. Circ Cardiovasc Imaging 2019. https://doi.org/10.1161/CIRCIMAGING.119.009404.
16. Nucifora G, Muser D, Tioni C, Shah R, Selvanayagam JB. Prognostic value of myocardial deformation imaging by cardiac magnetic resonance feature-tracking in patients with a first ST-segment elevation myocardial infarction. Int J Cardiol 2018. https://doi.org/10.1016/j.ijcard.2018.05.082.
17. Ogawa R, Kido T, Nakamura M, Kido T, Kurata A, Miyagawa M, et al. Diagnostic capability of feature-tracking cardiovascular magnetic resonance to detect infarcted segments: a comparison with tagged

magnetic resonance and wall thickening analysis. Clin Radiol 2017. https://doi.org/10.1016/j.crad.2017.05.010.

18. Morais P, Marchi A, Bogaert JA, Dresselaers T, Heyde B, D'Hooge J, et al. Cardiovascular magnetic resonance myocardial feature tracking using a non-rigid, elastic image registration algorithm: assessment of variability in a real-life clinical setting. J Cardiovasc Magn Reson 2017. https://doi.org/10.1186/s12968-017-0333-y.
19. Dobrovie M, Barreiro-Pérez M, Curione D, Symons R, Claus P, Voigt JU, et al. Inter-vendor reproducibility and accuracy of segmental left ventricular strain measurements using CMR feature tracking. Eur Radiol 2019;29:6846–57. https://doi.org/10.1007/s00330-019-06315-4.
20. Masci PG, Bogaert J. Post myocardial infarction of the left ventricle: the course ahead seen by cardiac MRI. Cardiovasc Diagn Ther 2012. https://doi.org/10.3978/j.issn.2223-3652.2012.04.06.
21. Rajiah P, Desai MY, Kwon D, Flamm SD. MR imaging of myocardial infarction. Radiographics 2013;33:1383–412. https://doi.org/10.1148/rg.335125722.
22. Mercado MG, Smith DK, McConnon ML. Myocardial infarction: Management of the subacute period. Am Fam Physician 2013.

Tables

Table 1 – Demographic characteristics: patients vs. controls

	acute infarcts (n=57)	controls (n=28)	p-values	acute infarcts	follow-up	p-values
Patient demographics				n= 32		
Sex (male/female)	42/15	26/2		23/9		
Age (years)	61± 12 [35-83]	47 ± 8 [44-69]	0.2	52 ± 7 [35-66]		
Height (m)	1.69 ± 12 [1.68-1.94]	1.65 ± 15 [1.57-1.9]	0.3	1.71 ± 8 [1.68-1.8]		
Weight (kg)	79.8 ± 15 [68-103]	76.4 ± 10 [68-94]	0.7	77.2 ± 11 [68-90]		
BMI	27 +/- 5 [25-31]	25 ± 3 [22-30]	0.5	27 +/- 4 [24-29]		
Left ventricular morphology						
LVEDV (ml,117-200)	191 ± 23 [104-291]	166 ± 37 [81-215]	0.1	172 ± 19 [114-211]	184 ± 27 [145-288]	0.2
LVESV (ml, 31-76)	81 ± 32 [45-195]	87 ± 24 [31-110]	0.4	80 ± 29 [38-160]	86 ± 26 [49-195]	0.8
LVSV (ml, 77-133)	83 ± 15 [57-101]	90 ± 17 [60-111]	0.6	89 ± 18 [57-115]	72 ± 18 [59-103]	0.5
LVEF (%, > 52)	50 ± 8 [28-62]	57 ± 4 [54-69]	0.4	47 ± 10 [50-62]	51 ± 8 [18-49]	0.2
LV Mass (g, 51-87)	60 ±14 [31-95]	52± 8 [37-90]	0.5	60 ±10 [37-95]	53 ± 8 [37-91]	0.6
Global strain						
GPCS (%)	-10.3 +/- 3	- 20.1 +/- 2	0.01	-10.6 +/- 2	- 9,5 +/- 3	0.7
GPLS (%)	-10.7 +/- 5	- 18.6+/- 2	0.04	-10.2 +/- 5	-10.9 +/- 5	0.8
GPRS (%)	27.9 +/- 5	39.2 +/- 5	0.01	26.8 +/- 6	29.8 +/- 4	0.2
Infarcts						
Infarcted segments	189/896	0	-	118/512	118/512	-
Scar burden (%)	23.4 ± 6 [8-59]	0	-	25.1 ± 5 [12-56]	20.7 ± 4 [5-48]	0.6
Myocardial oedema only	27	0	-	10	0	-

BMI= body mass index, *LVEDV*= left ventricular end-diastolic volume, *LVESV*= left ventricular end-systolic volume, *LVSV*= left ventricular stroke volume, *LVEF*= left ventricular ejection fraction; GPCS/GPLS/GPRS = global circumferential/longitudinal/radial strain; values in round brackets are standard, cohort specific LV values; values in square brackets represent the value range

Table 2 – Interobserver agreement

	ICC acute	ICC follow up
Global strain		
GPCS	0.902 [95% CI:0.878-0.930]	0.916 [95% CI:0.882-0.941]
GPLS	0.850 [95% CI:0.817-0.879]	0.878 [95% CI:0.804-0.929]
GPRS	0.893 [95% CI:0.851-0.939]	0.897 [95% CI:0.878-0.947]
Segmental strain		
SPCS	0.899 [95% CI:0.862-0.922]	0.903 [95% CI:0.869-0.934]
SPLS	0.732 [95% CI:0.711-0.749]	0.719 [95% CI:0.701-0.747]
SPRS	0.804 [95% CI:0.793-0.869]	0.817 [95% CI:0.797-0.902]

GPCS/GPLS/GPRS = global circumferential/longitudinal/radial strain; SPCS/SPLS/SPRS= segmental circumferential/longitudinal/radial strain, ICC = intraclass correlation coefficient

Figures

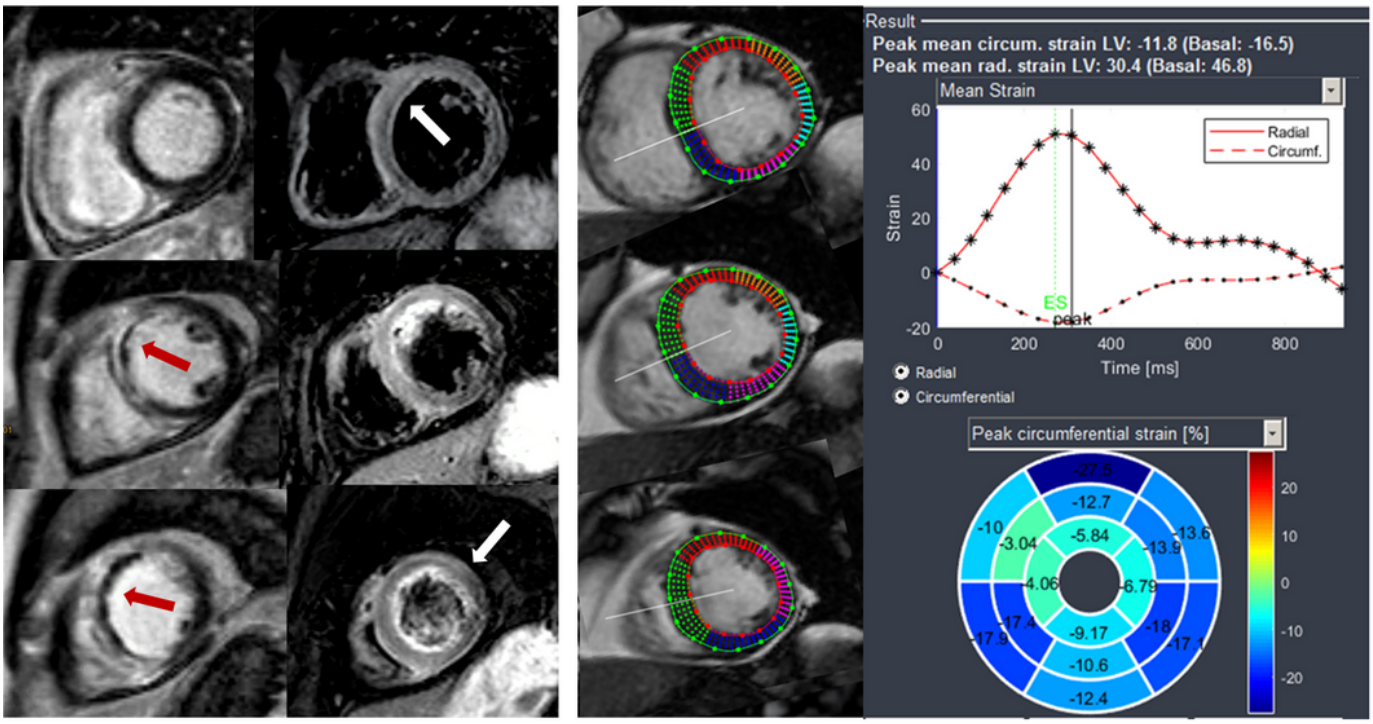

A

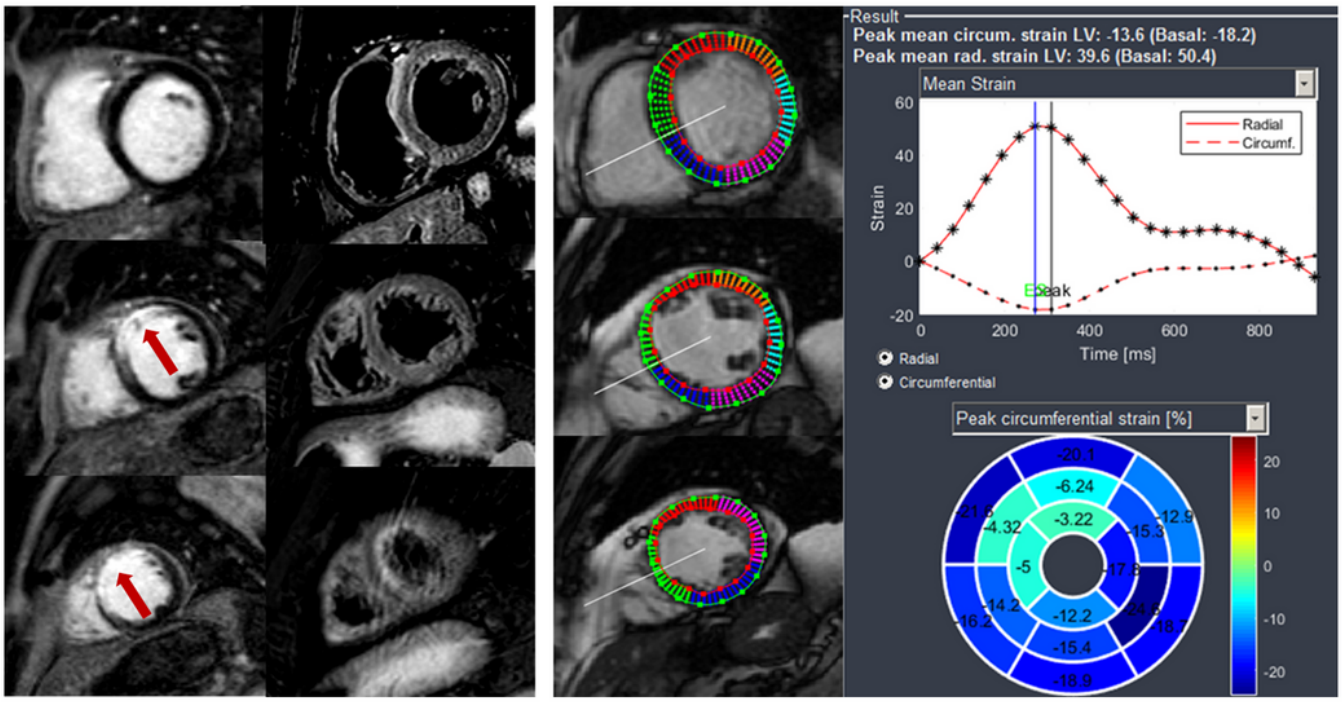

B

Figure 1

a – 48-year old patient 2 days after infarction of the anteroseptal wall Left column: LGE in segment 8, 13,14 (red arrows), concomitant edema extends additionally into segments 2,7,16 (white arrows). Right column: Endo- and epicardially contoured basal, midventricular and apical cine short axis slices prepared for circumferential strain calculations with polar plot strain map. Infarcted segments display reduced SPCS values in the strain map. b – 48-year old patient 35 days after infarction of the anteroseptal wall

Same patients as in Figure 1a. Left column: LGE in segment 8, 13,14 (red arrows), no concomitant edema; right colum: Endo- and epicardially contoured basal, midventricular and apical cine short axis slices prepared for circumferential strain calculations with polar plot strain map. Infarcted segments display reduced SPCS values in the strain map.

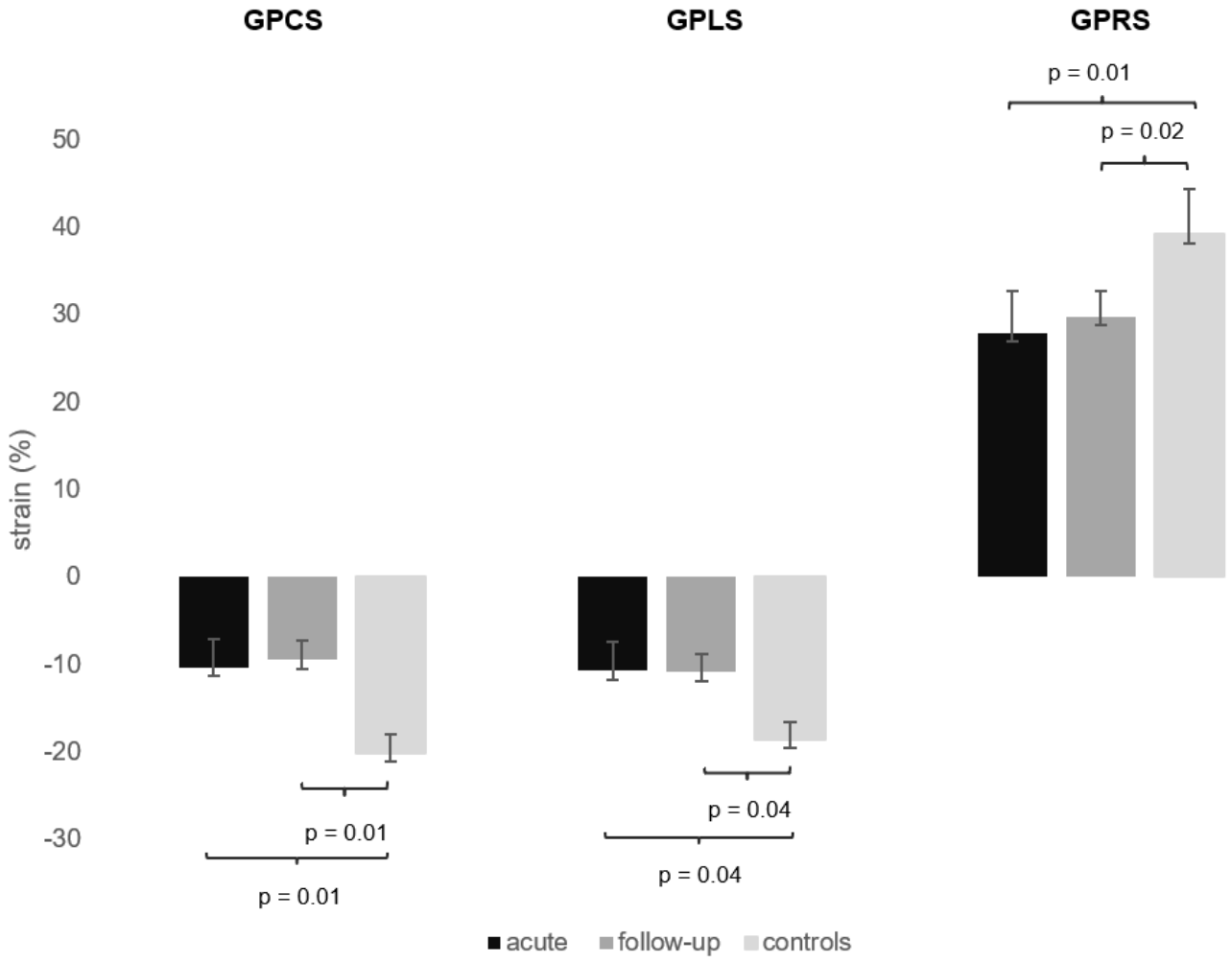

Figure 2

Global strain values in patients and healthy controls While GPCS, GPLS and GPRS values were very similar comparing both imaging time points, they were significantly impaired compared to healthy controls. GPCS = global peak circumferential strain, GPLS = global peak longitudinal strain, GPRS = global peak radial strain

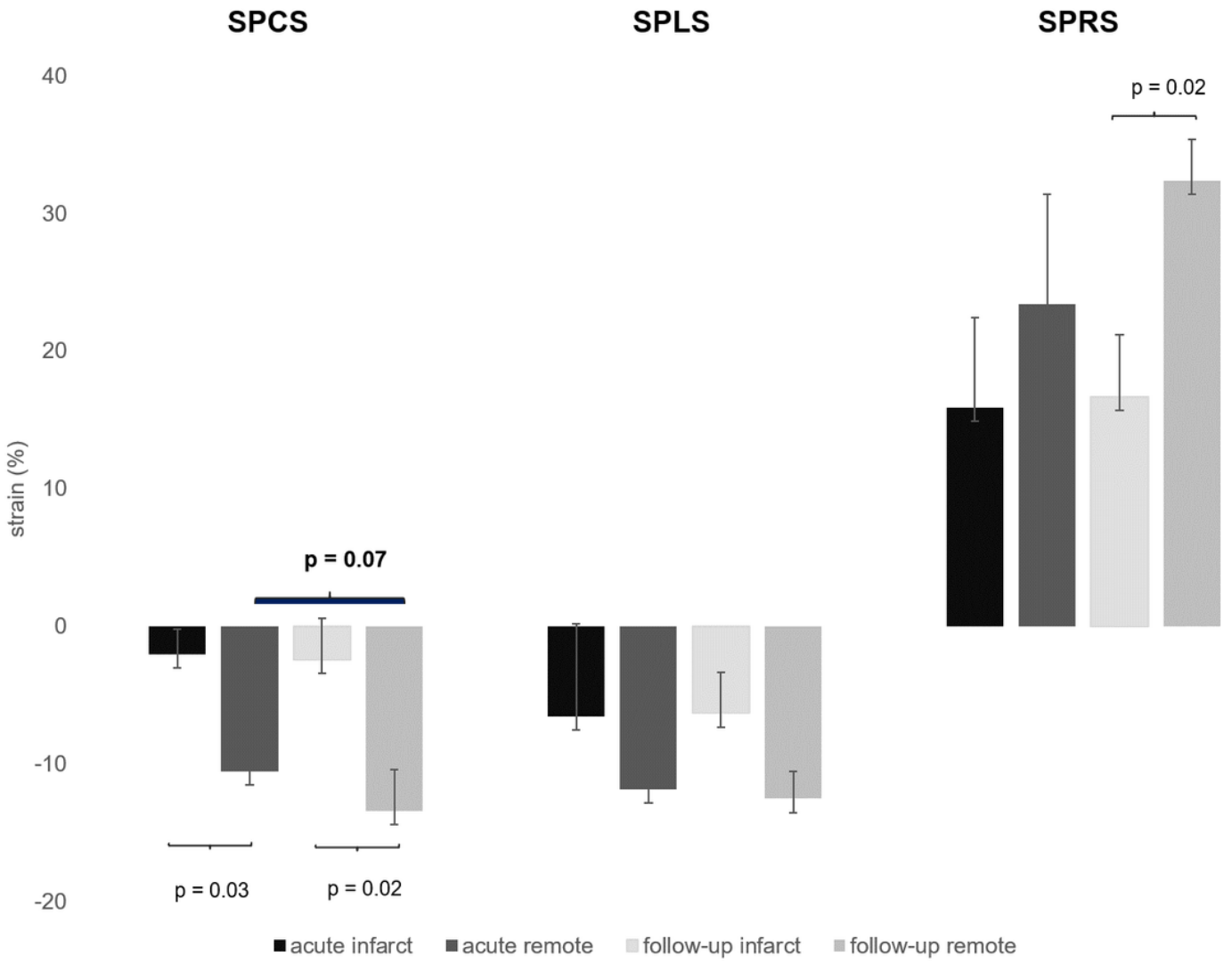

Figure 3

Segmental strain values for infarcted segments and remote myocardium in acute and follow-up CMR Significantly different values between infarcted and remote myocardium can be detected in SPCS for both imaging time points as well as in SPRS in the follow-up exams. SPCS = segmental peak circumferential strain, SPLS = segmental peak longitudinal strain, SPRS = segmental peak radial strain

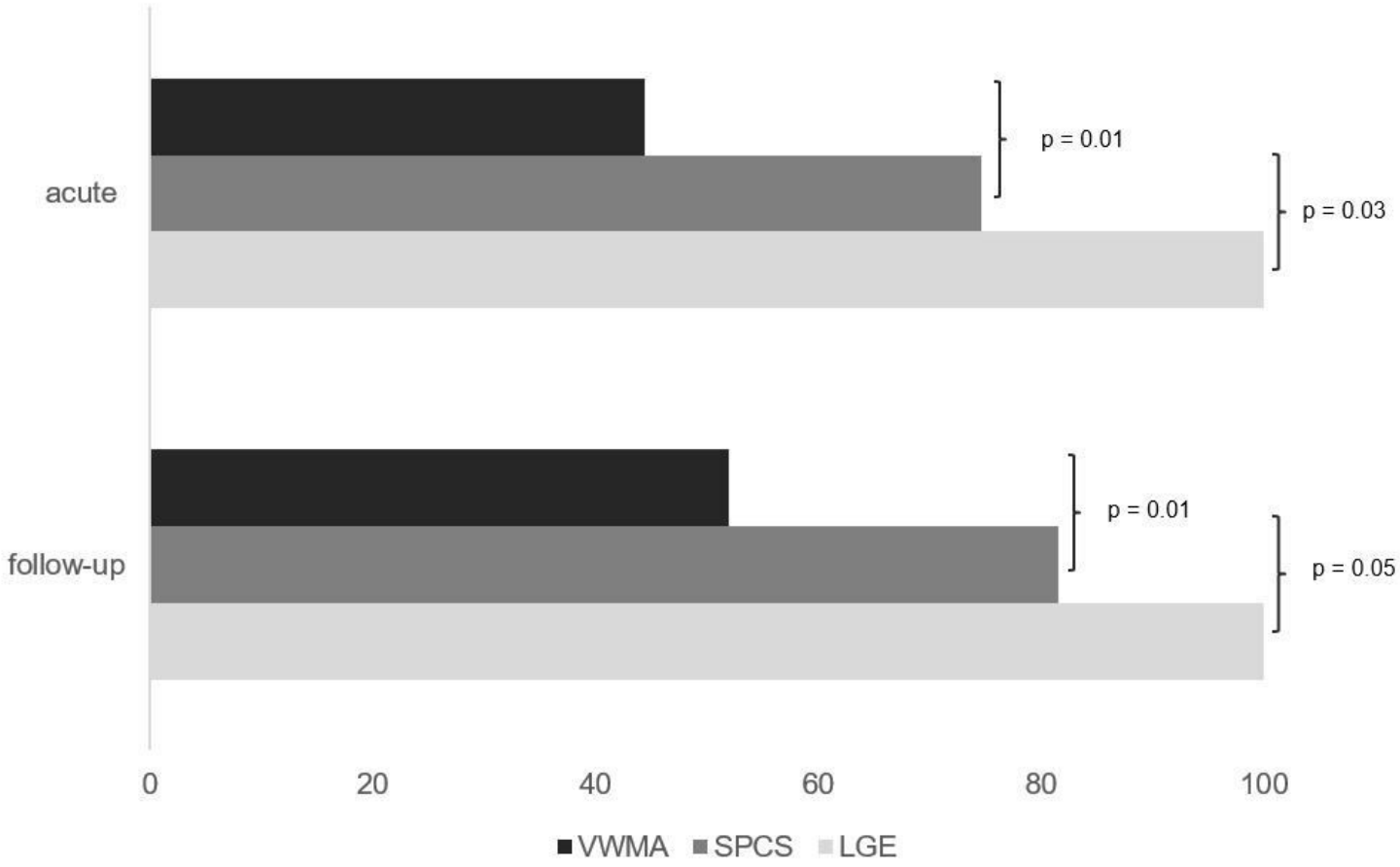

Figure 4

Localization of infarcted segments showed in segmental circumferential strain calculations Segmental strain calculations showed significantly more infarcted segments than visual assessment of wall motion abnormalities in cine images and this was significant in both imaging time points. In follow-up exams more infarcted segments were found in visual assessment of wall motion compared to acute infarcts (52% vs. 44.4%). LGE = late gadolinium enhancement, SPCS = segmental peak circumferential strain, VWMA = visual wall motion assessment

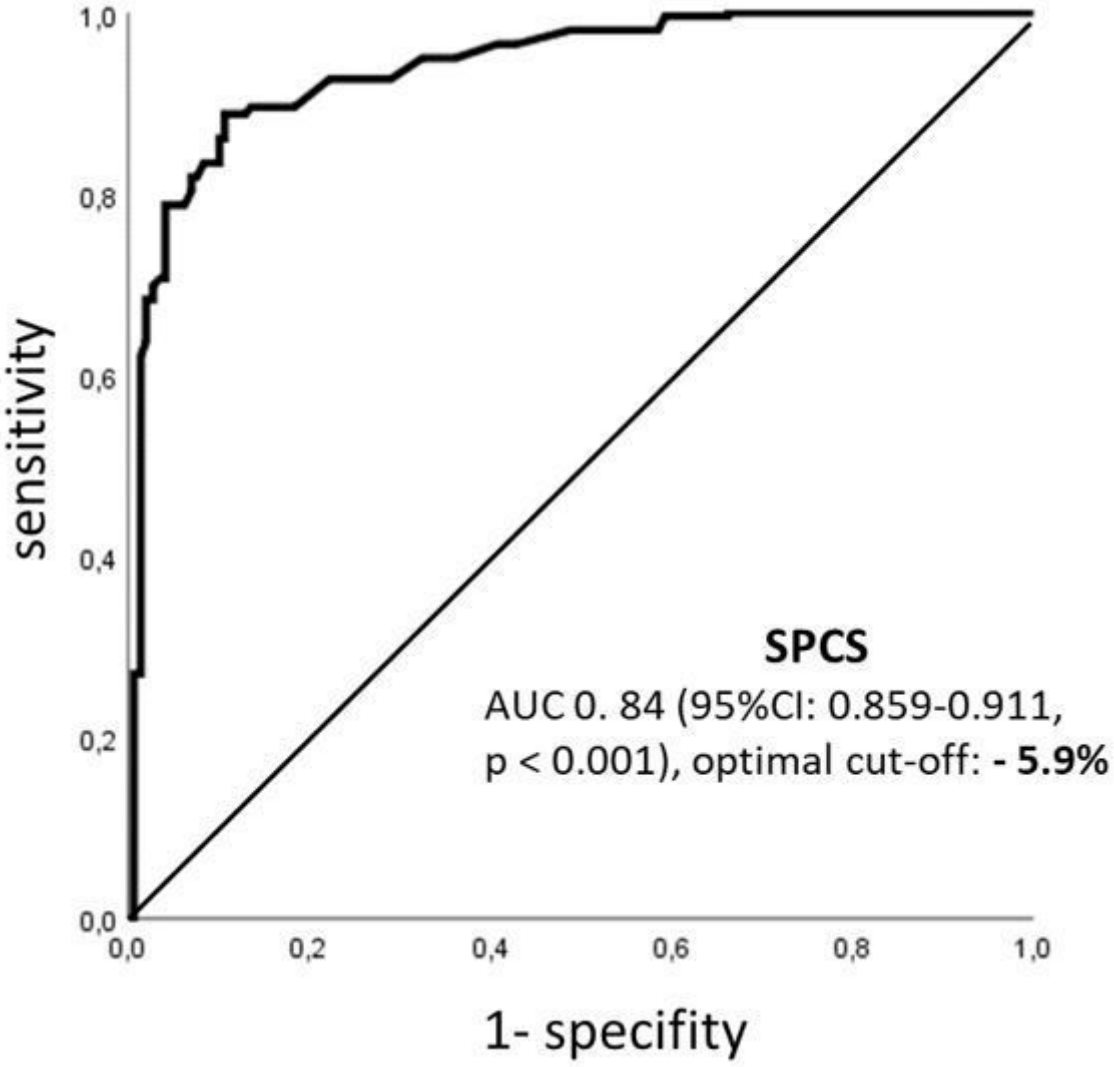

Figure 5

ROC curve for distinguishing infarcted and remote myocardium based on strain parameters Below a SPCS value of -5,9 % (sensitivity of 86,2 %, specificity of 83,5%) segments are considered infarcted. ROC= Receiver operating characteristic, SPCS= segmental peak circumferential strain